

## Structure Determination of $\text{Ca}_4\text{Fe}_2\text{Ti}_2\text{O}_{11}$ by Electron Microscopy and Crystallographic Image Processing

SVEN HOVMÖLLER, XIAODONG ZOU, AND DA NENG WANG

*Structural Chemistry, University of Stockholm, S-106 91 Stockholm, Sweden*

AND JOSE MARIA GONZÁLEZ-CALBET AND MARIA VALLET-REGÍ

*Inorganic Chemistry, Complutense University, Madrid 280 40, Spain*

Received May 4, 1988

The crystal structure of  $\text{Ca}_4\text{Fe}_2\text{Ti}_2\text{O}_{11}$  has been determined by high-resolution electron microscopy and crystallographic image processing. The space group is *Pnma*. The Perovskite-type structure is composed of  $\text{MeO}_6$  octahedra and  $\text{MeO}_4$  tetrahedra, arranged as OOOTOOT along the long *b*-axis of the crystals. © 1988 Academic Press, Inc.

### Introduction

Perovskite-related oxides,  $\text{AMo}_{3-y}$  are now at the center of interest because some of them have shown superconducting properties at high temperatures (1, 2). Since Wadsley (3) predicted the existence of ordered phases between the perovskite ( $\text{AMo}_3$ ) and the brownmillerite ( $\text{AMo}_{2.5}$ ) structural types, many efforts have been made to obtain such materials. A detailed knowledge of the atomic structures of these materials is essential for a better comprehension of their properties.

Many of these compounds are difficult to prepare as single crystals large enough to be studied by X-ray diffraction. For these high-resolution electron microscopy (HREM) is the most suitable method for obtaining structural information at the unit cell level. The perovskite-related oxide  $\text{Ca}_4\text{Fe}_2\text{Ti}_2\text{O}_{11}$ , the  $n = 4$  member in a series having the general formula  $A_nM_nO_{3n-1}$  is one of these cases.

In a previous study of this compound by

HREM, electron diffraction, and X-ray powder diffraction (4) a structural model was proposed, with alternating  $\text{MeO}_6$  octahedra and  $\text{MeO}_4$  tetrahedra, arranged as OOOTOOT. . . The space group was not determined, but the crystals were considered orthorhombic with  $a = 5.437(1)$ ,  $b = 30.22(1)$ , and  $c = 5.489(1)$  Å.

It has been shown that HREM combined with crystallographic image processing (CIP) can be used to determine coordinates of metal atoms in oxides with an accuracy of about 0.1 Å (5, 6). In order to determine if the earlier proposed model of  $\text{Ca}_4\text{Fe}_2\text{Ti}_2\text{O}_{11}$  was correct, we applied CIP on the HREM images of the structure.

### Materials and Methods

The preparation of  $\text{Ca}_4\text{Fe}_2\text{Ti}_2\text{O}_{11}$  and the electron microscopy were described earlier (4). The same HREM images and electron diffraction patterns that were published in (4) were used in the present investigation. In addition the (*hk*0) electron diffractogram

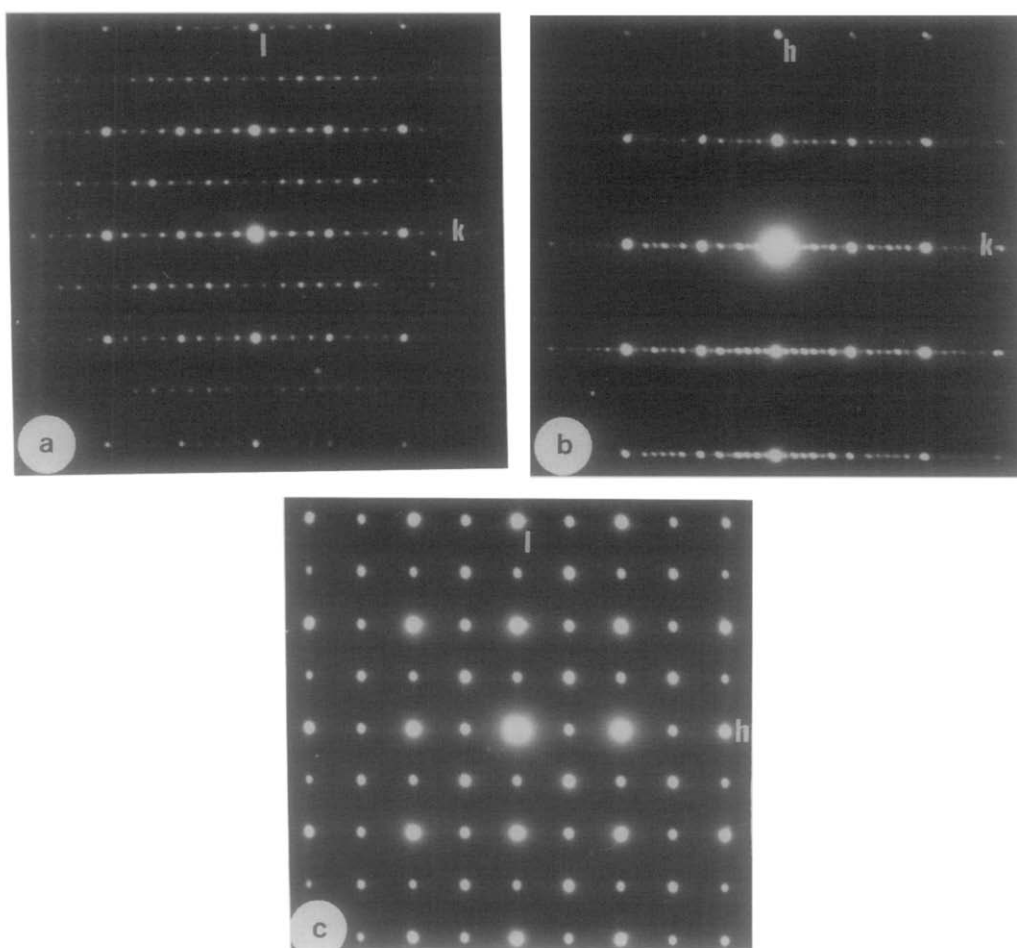


FIG. 1. Electron diffraction patterns of  $\text{Ca}_4\text{Fe}_2\text{Ti}_2\text{O}_{11}$ . (a)  $(0kl)$ , showing systematic absences for  $k+l$  odd; (b)  $(hk0)$  with absences for  $h$  odd; and (c)  $(h0l)$  with no absences, but with odd axial reflections weaker than the even ones.

was used here for space group determination (Fig. 1).

The two HREM images taken along two different crystal axes ( $a$  and  $c$ ) were first analyzed in an optical diffractometer. In the optical diffractometer the resolution and crystal symmetry were studied over the whole areas of the electron micrographs, and the thinnest areas were selected for digitization and image processing.

The axial projections (Figs. 2 and 3) had

very small areas at the edges which were selected for digitization.

The digitization and calculation of Fourier transforms of the images were done as described earlier (5). The images were scanned using a Joyce-Loebl flat-bed microdensitometer MDM 6 with raster size  $40 \times 40 \mu\text{m}$  and an array of  $256 \times 256$  raster points, giving a total area of about  $1 \text{ cm}^2$ . For the two projections the scanned areas were further trimmed on the computer, so

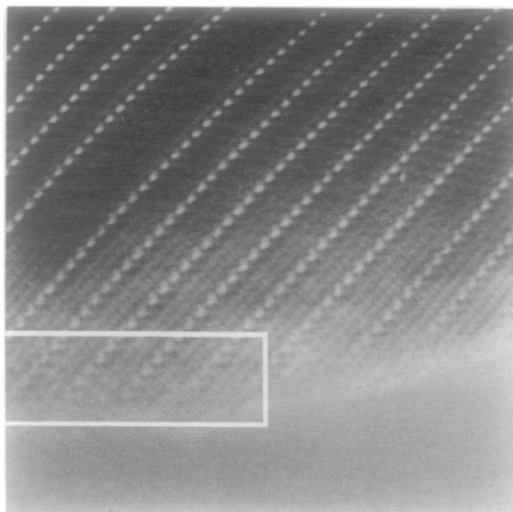


FIG. 2. HREM image of  $\text{Ca}_4\text{Fe}_2\text{Ti}_2\text{O}_{11}$  projected along the  $a$ -axis. Only the thin area indicated was selected for CIP.

that only very thin areas near the edges were used. These areas were about 10 unit cells ( $50 \text{ \AA}$ ) from the edge and in. Fourier transforms of the digitized areas were calculated and amplitudes and phases extracted from the Fourier transforms using a VAX 11/750 computer.

Electron diffraction intensities were obtained by scanning the electron diffraction patterns in the microdensitometer. Symmetry-related reflections were averaged. Amplitudes were obtained as the square roots of the intensities.

The crystal symmetry was determined mainly from the electron diffraction patterns but with additional information from the calculated Fourier transforms, which, in addition to the amplitudes obtainable from electron diffraction patterns, also contains the phase information.

The two processed HREM images were both taken along directions for which the projections possibly were centrosymmetric. For such projections all phases are either  $0^\circ$  or  $180^\circ$ , provided the phase origin is

on a symmetry center in the unit cell. The phase origins are initially at the center of the scanned area, not necessarily coinciding with a symmetry center. A computer program searches throughout one unit cell in order to find a possible symmetry center. Once this has been established the phases are shifted to be related to this origin. The phase residual, i.e., the phase deviation from the values expected for a certain symmetry, is calculated. When the phase residual indicated a centrosymmetric projection, all phases were set to be exactly  $0^\circ$  or  $180^\circ$ . Amplitudes of symmetry-related reflections such as  $(hkl)$  and  $(h\bar{k}l)$  were averaged. Amplitudes were taken either from the calculated Fourier transforms, or from the diffractograms. Data outside  $2.7 \text{ \AA}$  resolution was deleted.

The final projected density maps were calculated from the symmetrized amplitudes and phases and displayed on a computer graphics monitor.

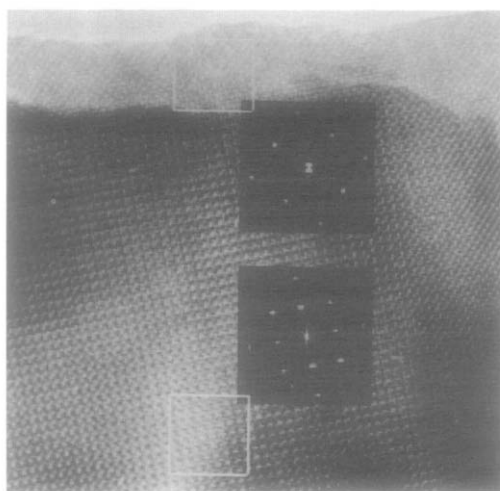


FIG. 3. HREM image of  $\text{Ca}_4\text{Fe}_2\text{Ti}_2\text{O}_{11}$  projected along the  $b$ -axis. Two small areas and their corresponding computer-calculated Fourier transforms are indicated. The forbidden axial reflections  $(100)$  and  $(001)$  are absent in the thin edge, but appear in the thicker part of the crystal, obviously as an effect of multiple scattering.

## Results and Discussion

### Space Group Determination

The space group was determined to be  $Pnma$  (No. 62) in (7) from the following observations. The  $(0kl)$  electron diffraction pattern (Fig. 1a) shows systematic absences for  $(k+l)$  odd reflections. The  $(hk0)$  diffraction pattern (Fig. 1b) has absences for  $h = 2n + 1$  and also  $(0k0)$  for  $k$  odd.

The  $(h0l)$  diffraction pattern (Fig. 1c) shows no systematic absences in the electron diffraction pattern, not even the axial reflections that were absent in the other projections. The optical diffraction proved that the presence of the forbidden odd axial reflections was caused by multiple diffraction. In the thin edge of these crystals (Fig. 3) the odd axial reflections were indeed ab-

sent, but they appeared in the thicker areas. The electron diffraction pattern has contributions from a relatively large part of the crystal, including both the thin edge and thicker parts, and so has intensity also in the forbidden reflections.

In summary the conditions for diffraction were  $(hkl)$  all orders,  $(0kl)$   $k + l = 2n$ ,  $(hk0)$   $h = 2n$ , and  $(h0l)$  all orders. This leaves two possible space groups,  $Pnma$  (No. 62) and  $Pn2_1a$  (No. 33). These two space groups have the same systematic absences and cannot be separated by information obtained from diffraction patterns. They differ only in that  $Pnma$  is centrosymmetric. It can be seen from Table I that the phases of the reflections in the  $(0kl)$  projection are close to 0 or  $180^\circ$ , with an average phase residual of  $20.3^\circ$ . If the crystal is noncentro-

TABLE I  
AMPLITUDES AND PHASES OF  $\text{Ca}_4\text{Fe}_2\text{Ti}_2\text{O}_{11}$  AS DERIVED BY CRYSTALLOGRAPHIC IMAGE PROCESSING OF HREM IMAGES, AND AMPLITUDES OBTAINED FROM THE ELECTRON DIFFRACTION PATTERNS

Indices ( <i>h k l</i> )	Amplitudes from electron diffraction	Amplitudes and phases from Fourier trans- forms of HREM image		Symmetrized phases
0 2 0	147	95	196	180
0 4 0	125	205	32	0
0 6 0	130	186	192	180
0 8 0	186	147	145	180
0 10 0	86	36	200	180
0 1 1	42	58	28	0
0 1 -1	42	67	173	180
0 3 1	80	106	217	180
0 3 -1	80	89	359	0
0 5 1	105	102	54	0
0 5 -1	105	85	192	180
0 7 1	75	133	150	180
0 7 -1	75	71	0	0
0 0 2	219	116	180	180
2 0 0	151	112	177	180
1 0 1	126	120	31	180
1 0 -1	126	207	358	180
0 0 2	146	110	216	180

Note. The different sets of amplitudes were put on the same scale. The last four reflections are from the  $[010]$  projection; the others are from the  $[100]$  projection.

symmetric,  $Pn2_1a$ , then the phase values of most reflections are not restricted to  $0^\circ$  or  $180^\circ$ , but each pair  $(0kl)$  and  $(0k\bar{l})$  must have the same phase. The phase residual for  $Pn2_1a$  symmetry was  $16.7^\circ$ .

When in doubt about the true space group of a crystal, the one with the highest symmetry should be chosen. Only when better data is available, proving a significant deviation from the higher symmetry, is it correct to assign the space group with the lower symmetry to the crystal. In the present case the phase residual for the lower symmetry ( $Pn2_1a$ ) was not significantly lower than that for the higher symmetry ( $Pnma$ ). This indicates that the crystal is centrosymmetric, having the space group  $Pnma$ , and this symmetry was then imposed on the data.

### Crystallographic Image Processing

The processed edge of the  $[100]$  projection (area indicated in Fig. 2) contains some 10 by 5 unit cells (50 by 150 Å). The amplitudes and phases of the scanned area, after shifting the phases to the proper origin, are shown in Table I. Pairs of  $(0kl)$  and  $(0k\bar{l})$  reflections should have phase values differing by  $180^\circ$ .

The only difficult phase to assign is that of  $(002)$ . It must be included in the data set, since without it the resolution in the  $c$  direction is very poor, and the octahedra are not resolved. The  $d$  value of  $(002)$  is 2.72 Å, very close to the resolution limit of the electron microscope (2.7 Å). For an image taken close to Scherzer focus, the amplitude of the  $(002)$  reflection will be greatly

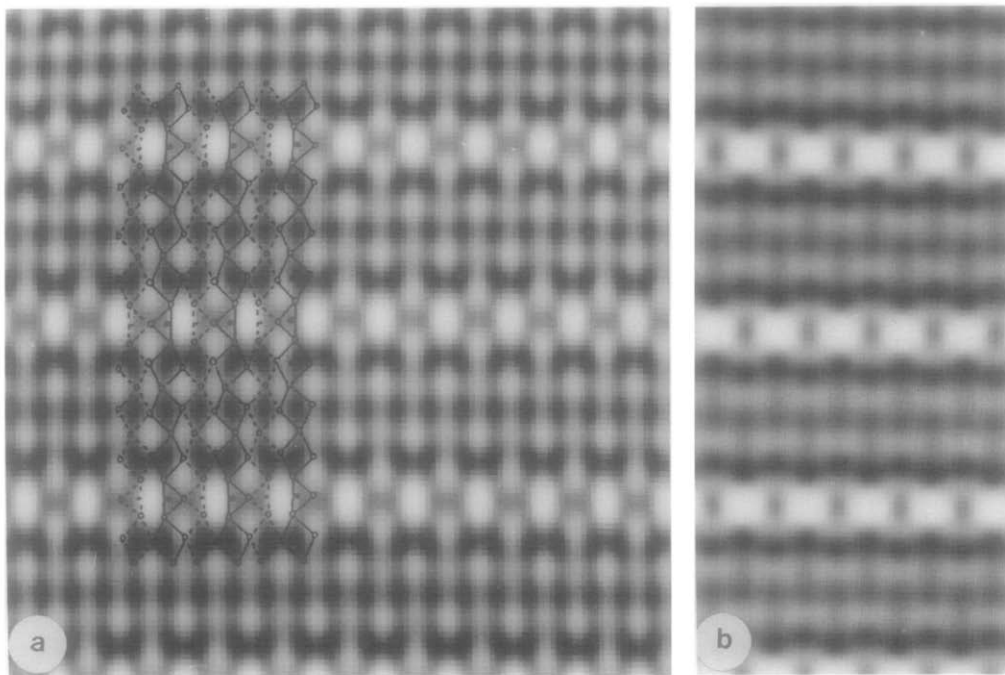


FIG. 4. The structure of  $\text{Ca}_4\text{Fe}_2\text{Ti}_2\text{O}_{11}$  projected down the  $a$ -axis, after applying CIP on the HREM image of Fig. 2. The phases used in (a) are the symmetrical phases shown in Table I. The amplitudes are those from the electron diffraction pattern. The same data was used in (b), except that the phase of the  $(002)$  reflection was reversed; i.e.,  $0^\circ$  instead of  $180^\circ$  as in (a). The structural model of  $\text{Ca}_4\text{Fe}_2\text{Ti}_2\text{O}_{11}$  as proposed in (4) is overlaid on the correct structure seen in (a).

attenuated. The phase of (002) can be correct or reversed depending on very small shifts in defocus, causing the first crossover of the contrast transfer function to come outside or inside this reflection. For this reason the true phase of the (002) reflection could not be determined in this case. Thus we calculated two different density maps, using the well-determined phases mentioned above, and the two possible phase values of the (002) reflection,  $0^\circ$  and  $180^\circ$ . The two density maps are shown in Fig. 4. Only one of them (Fig. 4a) gives a chemically interpretable structure, and is therefore considered to be the correct one.

Density maps were calculated using the centrosymmetric phases shown in Table I and the two different sets of amplitudes, namely those extracted from the Fourier transform of the HREM image and from the electron diffraction pattern. The two density maps were nearly identical.

The [010] projection contained only four reflections within the resolution limit. The density map calculated from these reflections showed the network of octahedra at  $(0, y, 0)$  and  $(\frac{1}{2}, y, \frac{1}{2})$ .

### Description of the Structure

The [010] projection shows a net of octahedra, interrupted by rows of tetrahedra. The sequence is OOOTOOOOT. . . and alternating rows of tetrahedra are oriented differently, such that the unit cell becomes centered and contains the sequence OOOTOOOT. A comparison with the

model proposed earlier (4) shows that the predicted model was correct (Fig. 4). Atomic coordinates for the Fe and Ti atoms as obtained from this structure determination are shown in Table II. Since iron but not titanium can have a tetrahedral coordination the atoms in the tetrahedra must be Fe. Half the Fe atoms are thus in the tetrahedra, and the other half and all Ti atoms are in the octahedra. At the present level of resolution it is not possible to determine whether these metal atoms are ordered or statistically disordered among the octahedral sites. No density attributable to the Ca atoms could be seen. In perovskite ( $\text{CaTiO}_3$ ) and brownmillerite ( $\text{Ca}_2\text{Fe}_2\text{O}_5$ ) the Ca atoms are located in the spaces between the octahedra. Since  $\text{Ca}_4\text{Fe}_2\text{Ti}_2\text{O}_{11}$  can be described as an ordered intergrowth between two perovskite unit cells and one-half brownmillerite unit cell, the Ca atoms are expected to be located in the spaces between the octahedra and between the tetrahedra in this structure.

### Acknowledgments

This study was carried out with financial help from the Swedish Science Research Council (NFR) and Hasselblads stiftelse. S.H. acknowledges a grant from Consejo Superior de Investigaciones Científicas for investigations in Madrid.

### References

1. J. G. BEDNORZ AND K. A. MÜLLER, *Z. Phys. B* **64**, 189 (1986).
2. R. I. CAVA, B. BATTLOG, R. B. VAN DOVER, D. W. MURPHY, S. SUNSHINE, J. P. REMEIK, A. G. RIETMAN, S. ZAHORAK, AND G. P. ESPINOSA, *Phys. Rev. Lett.* **58**, 1676 (1987).
3. D. A. WADSLEY, in "Nonstoichiometric Compounds" (L. Mandelcom, Ed.), Chap. 3, p. 135, Academic Press, New York (1964).
4. J. M. GONZÁLEZ-CALBET AND M. VALI ET-REGÍ, *J. Solid State Chem.* **68**, 266 (1987).
5. S. HOVMÖLLER, A. SJÖGREN, G. FARRANTS, M. SUNDBERG, AND B.-O. MARINDER, *Nature (London)* **311**, 238 (1984).
6. D. X. LI AND S. HOVMÖLLER, *J. Solid State Chem.* **73**, 5 (1988).
7. T. HAHN, Ed. "International Tables for Crystallography," Vol. A, Reidel, Dodrecht (1983).

TABLE II  
COORDINATES FOR THE Fe AND Ti ATOMS  
IN  $\text{Ca}_4\text{Fe}_2\text{Ti}_2\text{O}_{11}$

Atom	x	y	z	Multiplicity
Fe (T)	0.000	0.250	-0.100	4 c m
Fe/Ti (O)	0.000	0.125	0.020	8 d 1
Fe/Ti (O)	0.000	0.000	0.000	4 a 1

Note. T = tetrahedral and O = octahedral coordination.